



OPEN

Pulmonary arteries in coelacanth shed light on the vasculature evolution of air-breathing organs in vertebrates

Camila Cupello^{1✉}, Gaël Clément², Marc Herbin³, François J. Meunier⁴ & Paulo M. Brito¹

To date, the presence of pulmonary organs in the fossil record is extremely rare. Among extant vertebrates, lungs are described in actinopterygian polypterids and in all sarcopterygians, including coelacanth and lungfish. However, vasculature of pulmonary arteries has never been accurately identified neither in fossil nor extant coelacanth due to the paucity of fossil preservation of pulmonary organs and limitations of invasive studies in extant specimens. Here we present the first description of the pulmonary vasculature in both fossil and extant actinistian, a non-tetrapod sarcopterygian clade, contributing to a more in-depth discussion on the morphology of these structures and on the possible homology between vertebrate air-filled organs (lungs of sarcopterygians, lungs of actinopterygians, and gas bladders of actinopterygians).

Vascular canals and/or spaces are rarely documented in fossil bones. They have been described using both traditional techniques, such as ground sections (e.g. the Devonian osteostracan agnathan *Norselaspis glacialis*¹), and advanced technologies such as synchrotron imaging. Regarding early vertebrates, phase contrast X-ray synchrotron imaging of an acanthothoracid placoderm from the Early Devonian of Canadian Arctic Archipelago has provided a detailed three-dimensional view of the skull vascularization and nerve canals². The same technique also revealed vascular spaces in other taxa, such as the vascular mesh of the interolateral plate of the placoderm *Compagopiscis croucheri* (Late Devonian of Gogo Formation, Western Australia) or the vascular architecture of the humerus of *Eusthenopteron*, a sarcopterygian fish close to tetrapods (Late Devonian of Québec, Canada)³. Among tetrapods, traces of fossil blood vessels (arteries and veins) were reported for instance in the nasal bone of *Discosauriscus austriacus* from the Early Permian of Czech Republic³, in a *Triceratops* skull from the Upper Cretaceous of Hell Creek Formation, Montana⁴, in whale bones from the Middle-Upper Miocene of Peru⁵, and in turtles from the Eocene of Germany and Miocene of Colombia⁶. These might represent internal moulds of the vascular walls or even the filling of the vascular channels⁵.

On the other hand, pulmonary vasculature (including traces such as internal moulds) has not been documented in vertebrate fossils to date. Pulmonary arteries and veins are documented in all groups of extant osteichthyans, except in Lepisosteidae (where the dorsal aorta serves as the afferent blood supply to the respiratory gas bladder), and in Chondrostei and Teleostei (which exhibit celiacomesenteric arteries)⁷. However, pulmonary arteries have never been properly described in any developmental stage of the extant coelacanth *Latimeria chalumnae*. This may be due to the challenge of visualizing vessels in x-ray microtomography (the unique effective non-invasive methodology to study all developmental stages of extant coelacanth) without the presence of a contrast solution or even to the reabsorption of vascularization in adult specimens of the extant coelacanth that possess a vestigial lung^{8–10}. Based on histological thin sections of the lung lumen, pulmonary arteries were first erroneously described due to a misconception involving the pulmonary bony plates that are located on the vestigial lung^{11,12}. More recently, these small and dense plates that surround the vestigial lung of *Latimeria chalumnae* were described as homologous to the calcified plates of Palaeozoic and Mesozoic coelacanth lungs¹¹.

¹Departamento de Zoologia, Instituto de Biologia-IBRAG, Universidade do Estado do Rio de Janeiro, Rio de Janeiro, RJ, Brazil. ²Département Origines & Evolution, Muséum national d'Histoire naturelle, UMR 7207 (MNHN–CNRS–Sorbonne Universités) Centre de Recherche en Paléontologie (CR2P), Paris, France. ³Département Adaptations du Vivant, Muséum national d'Histoire naturelle, UMR 7179 (CNRS–MNHN) Mécanismes Adaptatifs et Evolution (MECADEV), Paris, France. ⁴Département Adaptations du Vivant, Muséum national d'Histoire naturelle, UMR 8067 (CNRS–IRD–MNHN–Sorbonne Universités–UCN, UA), Laboratoire de Biologie des Organismes et des Ecosystèmes Aquatiques (BOREA), Paris, France. ✉email: camila.dc@gmail.com

Here we describe, for the first time, the presence of pulmonary vessels in both fossil and extant coelacanths. These new observations confirm the air-breathing function of the so-called calcified organ in fossil coelacanths and the regressed state of the so-called vestigial lung in extant coelacanths. Presence of pulmonary vessels within this group resolves a piece of the puzzle regarding the evolution of air-breathing in vertebrates.

Results

Identification of pulmonary vasculature in the fossil coelacanth *Macropoma mantelli* (Late Cretaceous, Chalk Formation, Lewes, England)

The calcified lung of the specimen NHMUK PV 4270 is a well-developed unpaired organ, tubular in shape. It displays large superimposed bony plates surrounding a wide lumen (Fig. 1). Plates are rounded in shape and present a concave internal side. The lung is preserved in a ventral, but distorted, position, without division into chambers and without constriction (Fig. 1a), as known in some other fossil coelacanths. The anterior opening is not visible. The specimen, its tomographic segmentation, and three-dimensional reconstructions (Fig. 1a and b), clearly display the impression of the dorsal aorta, the most important vessel of the circulatory system, along the entire length of the external surface of the lung (Fig. 1a and b). Two pulmonary arteries, both with the same length, are also present parallel, but internal to the lung lumen and recovered by the bony plates (Figs. 1c, 2).

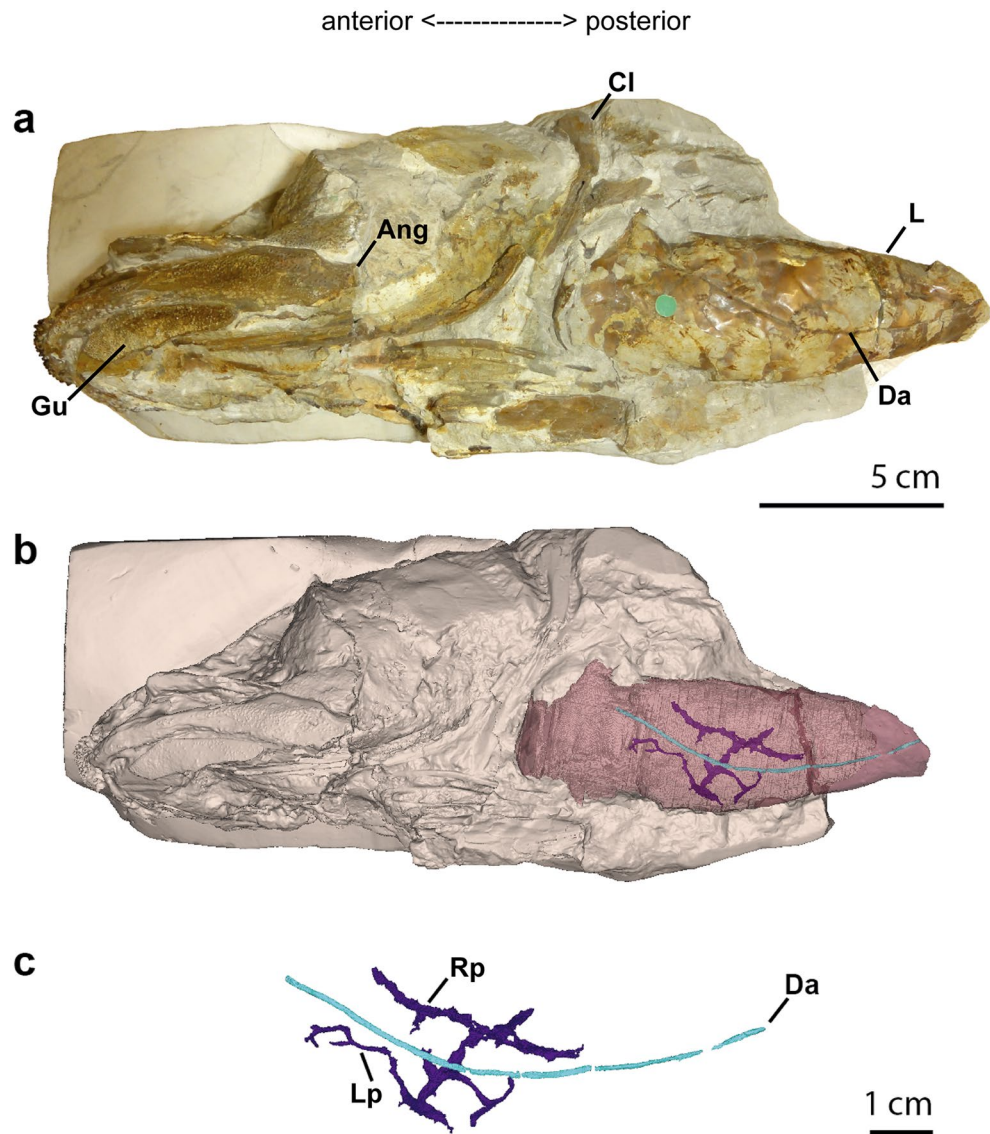


Figure 1. The pulmonary system of the Cretaceous coelacanth *Macropoma mantelli* NHMUK PV P 4270. (a) Photograph of specimen NHMUK PV 4270 in left lateral view. (b) Three-dimensional reconstruction of NHMUK PV 4270 with highlighting of the calcified lung, dorsal aorta and pulmonary arteries. (c) Close-up of the dorsal aorta and left and right pulmonary arteries. Pink, calcified lung; purple, pulmonary arteries; blue, dorsal aorta. *Ang* fragment of the angular bone, *Cl* cleithrum, *Da* dorsal aorta, *Gu* gular bone, *L* lung, *Lp* left pulmonary artery, *Rp* right pulmonary artery.

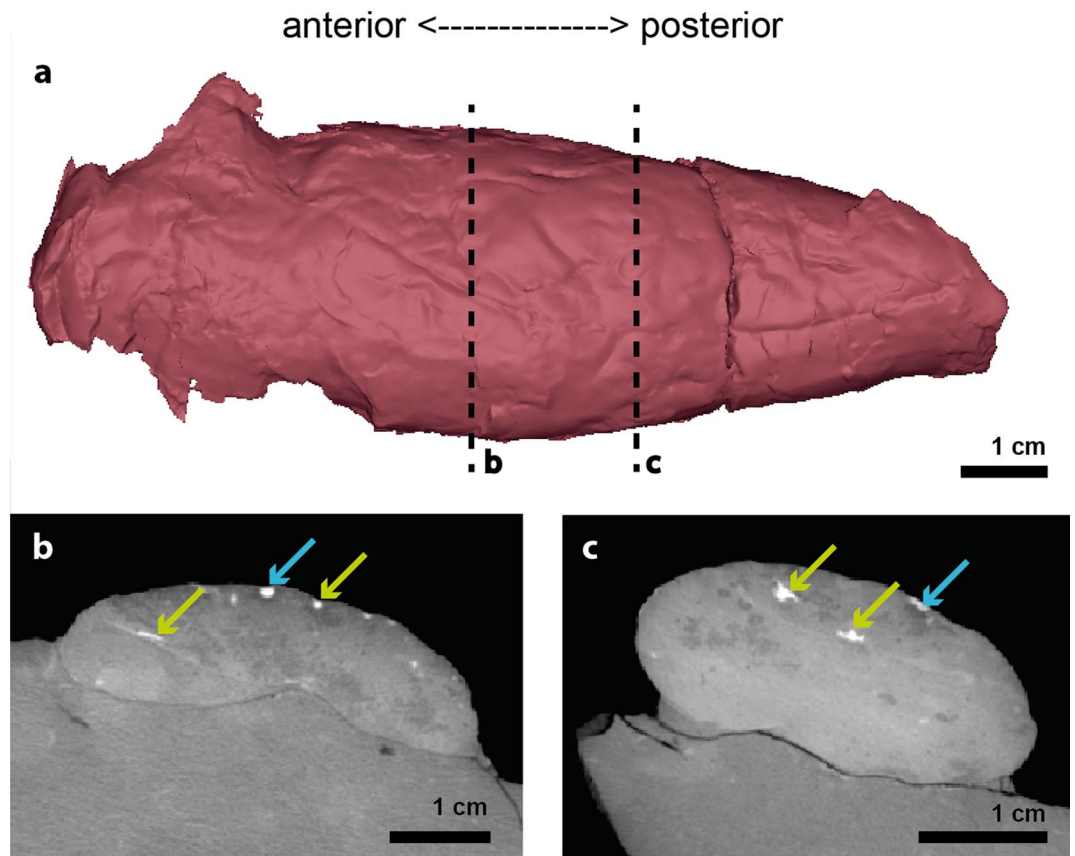


Figure 2. The calcified lung of *Macropoma mantelli* NHMUK PV P 4270. (a) Three-dimensional reconstruction of the calcified lung of the specimen. (b,c) Transverse sections of a high-resolution computerized axial tomography scan of NHMUK PV P 4270. Green arrows pointing to the pulmonary arteries internal to the lung lumen. Blue arrows, pointing to the dorsal aorta. Transverse tomography sections (b,c) corresponding to the successive dotted sections in (a).

These arteries are connected to each other by a transversal vessel. The pulmonary arteries give rise to branches of some arteries, as vascular channels (Fig. 1 c).

Evidence of pulmonary vasculature in a juvenile extant coelacanth *Latimeria chalumnae*

The lung of this juvenile coelacanth of 42.5 cm total length (specimen CCC 94) is unpaired, conical in shape and ventral to the oesophagus (Fig. 3). It is 2.157 cm long, corresponding to 15.88% of the length of the fatty organ and 5.13% of the length of the specimen (Fig. 3b). No bony plates are observed by X-ray tomography at this ontogenetic stage. The relative proportions between the lung and the total length (TL) of this specimen is lower in comparison to the same ratio in embryos and higher in comparison with the same ratio in adult specimens⁸.

The specimen CCC 94 was historically injected with colloidal barite for observation of the circulatory system¹², which reduced the quality of the tomography data for the soft tissues (Extended Data Fig. 1). However, this ancient injection has today enabled the visualization of the pulmonary arteries by X-ray tomography (usually not visible in coelacanth specimens without adding of colloidal barite) (Extended Data Fig. 1). The vestigial lung of CCC 94 is irrigated by two atrophied pulmonary arteries (Fig. 3c). Both pulmonary arteries run along the ventral surface of the vestigial lung. The dorsal aorta is not visible in this specimen, due to the artefacts generated by the massive injection of the contrast product. Indeed, barite strongly absorbs X-rays, resulting in a local hyper-signal that obscures the anatomical structures on tomographic data. No vascularization canals or branches were observed within the fatty organ or in the connective tissue surrounding it (Fig. 3d).

Discussion

Despite the rarity of preserved air-filled organs (AO¹³) in the fossil record, remains of pulmonary organs are known in an ornithuromorph bird, a salamander, a tadpole, as well as in almost all Palaeozoic and Mesozoic coelacanth families^{10,11,14–18}. Almost all well-preserved fossil coelacanths, except some taxa such as *Diplurus*, *Coccoderma suevicum* and juveniles of *Axelrodichthys araripensis*, show well preserved ossified plates in their abdominal cavity¹⁸. These bony plates are superimposed, multilayered, and separated from one another by unossified connective tissue, likely enabling their mobility for volume adjustment during air-breathing, as well as providing protection against hydrostatic pressure^{11,14}. The tubular structure, called the calcified organ, delimited

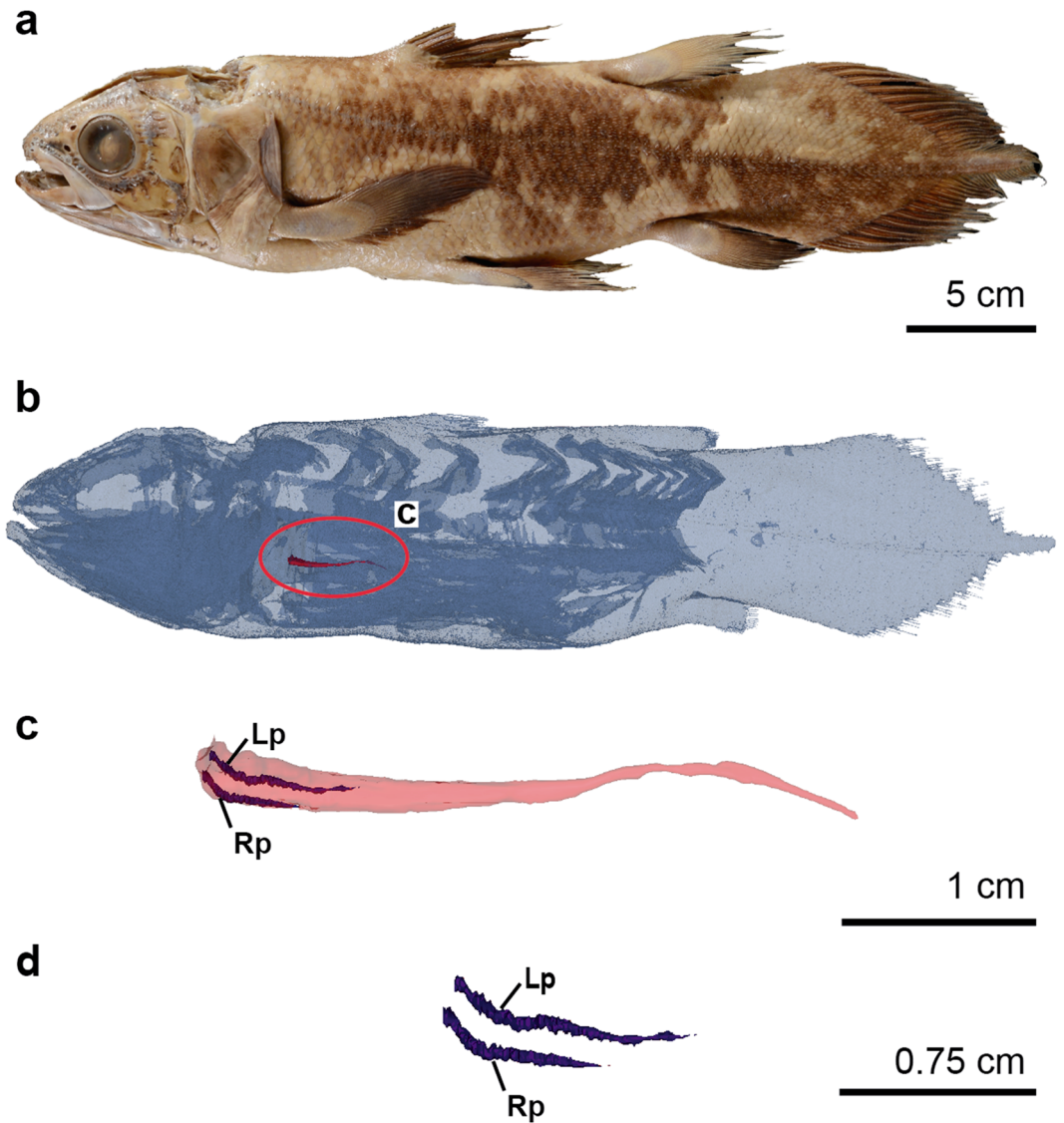


Figure 3. The pulmonary system of a juvenile specimen of the extant coelacanth *Latimeria chalumnae*. (a) Photograph of specimen CCC 94 (42.5 cm TL) in left lateral view. (b) Three-dimensional reconstruction of CCC 94. (c) Close-up of the three-dimensional reconstruction of the vestigial lung with left and right pulmonary arteries. (d) Close-up of the left and right pulmonary arteries. Pink, vestigial lung; purple, pulmonary arteries. *Lp* left pulmonary artery, *Rp* right pulmonary artery.

by a characteristic organization of these ossified plates has been recently considered as a structure constitutive of a functional lung in fossil coelacanths, homologous of the vestigial lung of extant coelacanths^{8,11,14}.

The Cretaceous coelacanth specimen of *Macropoma mantelli* here studied has a well-developed pulmonary organ with ossified plates surrounding it, as well as well-developed dorsal aorta, pair of pulmonary arteries, and supplementary pulmonary branches irrigating this air-breathing organ. The extant coelacanth *Latimeria chalumnae*, which inhabits moderately deep waters and do not perform aerial gas exchange, shows a vestigial lung with vestigial vasculature, consisting of only a pair of pulmonary arteries.

Coelacanths are key taxa for the understanding of the evolutionary steps of the air-breathing history in osteichthyans. These occurrences of pulmonary vasculatures in both fossil and extant coelacanths reinforce the homology hypothesis between the fossil calcified organ and the vestigial lung. They then shed light on the evolution of the pulmonary complex within the actinistian clade and particularly on the loss of air-breathing during deep-marine water adaptation of the *Latimeria* relatives. Presence of lung vascular systems in both fossil and extant coelacanths also provides new anatomical elements concerning the evolutionary history of the vascular supply of air-filled organs in osteichthyans and the homology between lungs and gas bladders (also called swimbladders or air bladders).

Lungs and gas bladders are morphologically distinct air-filled organs that can serve the functions of buoyancy control and/or air-breathing. The homology (or lack thereof) between these organs has been a

subject of discussion for almost 180 years^{19,20}. Since the nineteenth century, this discussion has been based on morphological and molecular analysis. Among the molecular aspects, some authors have proposed homology based on the co-expression of genes in both tetrapod lungs and actinopterygian gas bladders²¹, homologous genes shared between gas bladders and the human lung²², and the similar surfactant system between both air-filled organs²³. Morphologically, a homology was proposed based on different developmental stages of extant taxa that present a common origin from the posterior portion of the respiratory pharynx^{24–27}, their identical arterial supply^{7,13,25,28}, and their similar hydrostatic and/or respiratory function^{13,29}. Indeed, the only morphological difference between lungs and gas bladders is the ventral and dorsal origins from the foregut^{21,30}. Other characteristics previously used to differentiate both organs have been discarded in recent studies, as the lungs of actinopterygians and sarcopterygians, as well as the respiratory gas bladder of some actinopterygians, share certain morphological conditions^{9,10}. However, sharing the same function and/or morphology does not necessarily imply homology^{9,10,21,30}.

Based on our results, we confirm that extant and fossil coelacanths possess pulmonary arteries homologous to the same paired branches of the air-filled organs (including gas bladders) of other osteichthyans (Fig. 4). We also support the hypothesis that pulmonary arteries are a synapomorphy of Osteichthyes (Fig. 5). If considering the common arterial supply as an indicator of homology between lungs and gas bladders, our results may contribute to a better understanding of the homology of air-breathing organs in vertebrates (Fig. 5), but further studies may explore better this condition, as well as the anatomy of fossil and extant chondrichthyans to support the absence of pulmonary arteries in this group.

Methods

Specimen CCC 94 is a juvenile female of *Latimeria chalumnae* (42.5 cm TL) fished on a line in Comoro Islands in 1974³¹. This specimen was injected with colloidal barite to facilitate the observation of the circulatory system¹². It was scanned with long propagation phase-contrast synchrotron X-ray microtomography at the ID19 beamline of the European Synchrotron Radiation Facility (Grenoble, France) in a plastic tube filled with water and with

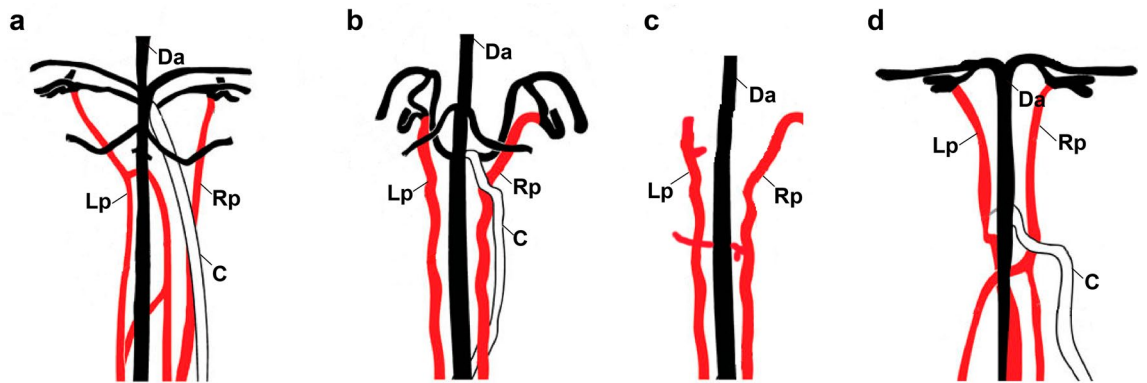


Figure 4. Schematic figure with a comparison of the pulmonary vascularization in Osteichthyes with potentially functional air-breathing organs (modified from Longo et al. 2013). (a) The actinopterygian *Polypterus senegalus*. (b) the holostean *Amia calva*. (c) the fossil coelacanth *Macropoma mantelli*. (d) the lungfish *Protopterus dolloi*. C celiacomesenteric artery, Da dorsal aorta, Lp left pulmonary artery, Rp right pulmonary artery.

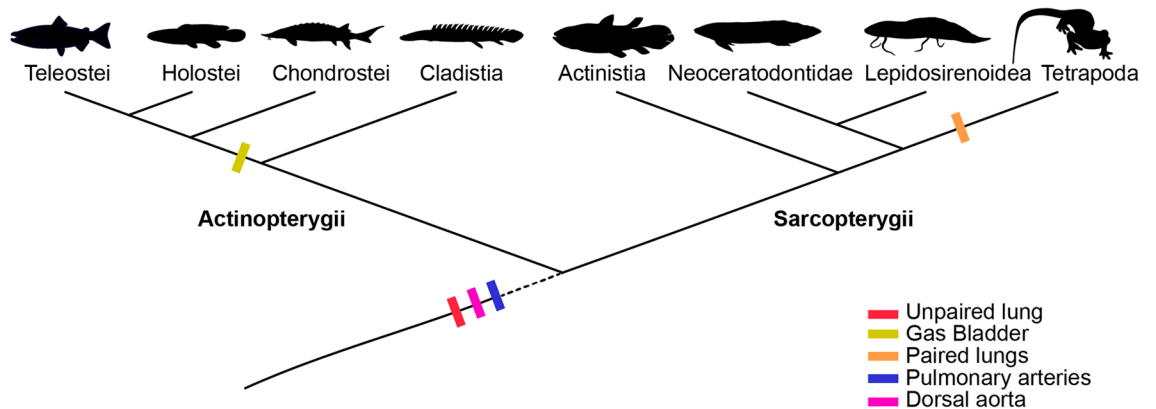


Figure 5. Schematic reconstruction of the evolutionary history of vertebrate lungs. Unpaired lung, pulmonary arteries and pulmonary arteries are plesiomorphies of Osteichthyes. Modified from Cupello et al.¹⁰. This figure was made with free silhouettes from PhyloPic.

a propagation distance of 13 m. The beam produced by the wiggler was filtered by 2 mm of aluminium and 15 mm of copper, at a gap of 30 mm, and resulting in an average detected energy of 170 keV with a bandwidth of 85 keV FWHM. The voxel size of the scan is 28.43 μm and the final reconstructions of 85.29 μm was obtained after binning. Slices were reconstructed with filtered back-projection algorithm, a single distance phase-retrieval process^{3,32}. Sub-scans were converted into 16-bit TIFF stacks and concatenated to generate a single complete scan. For more detail, see Cupello et al.⁸

Specimen NHMUK PV 4270 is an adult specimen of the fossil coelacanth *Macropoma mantelli* from the Late Cretaceous of Chalk Formation, Lewes, Sussex, UK. X-ray computed micro-tomography (μCT) scanning of this specimen was performed at the AST-RX Platform of the Muséum national d'Histoire naturelle, Paris, France. The voltage was 140 kV, current 350 mA, voxel size 127.85 μm and the view number was 1500.

For both specimens, segmentation and three-dimensional rendering were realized using the software MIMICS Innovation Suite 20.0 to 25.0 (Materialise) at the Laboratório de Ictiologia Tempo e Espaço of the Universidade do Estado do Rio de Janeiro.

Data availability

Data can be made available by the corresponding author upon request.

Received: 27 January 2024; Accepted: 30 April 2024

Published online: 09 May 2024

References

- Janvier, P., Percy, L. R. & Potter, I. C. The arrangement of the heart chambers and associated blood vessels in the Devonian osteostracan *Norselaspis glacialis*. A reinterpretation based on recent studies of the circulatory system in lampreys. *J. Zool.* **223**, 567–576. <https://doi.org/10.1111/j.1469-7998.1991.tb04388.x> (1991).
- Dupret, V., Sanchez, S., Goujet, D., Tafforeau, P. & Ahlberg, P. E. Bone vascularization and growth in placoderms (Vertebrata): The example of the premedian plate of *Romundina stellina* Örvig, 1975. *C. R. Palevol.* **9**, 369–375. <https://doi.org/10.1016/j.crpv.2010.07.005> (2010).
- Sanchez, S., Ahlberg, P. E., Trinajstić, K. M., Mirone, A. & Tafforeau, P. Three-dimensional synchrotron virtual paleohistology: A new insight into the world of fossil bone microstructures. *Microsc. Microanal.* **18**, 1095–1105. <https://doi.org/10.1017/S1431927612001079> (2012).
- Happ, J. W. & Morrow, C. M. Evidence of soft tissue associated with nasal and supraorbital horn cores, rostral and exoccipital of Triceratops. *J. Vertebr. Paleontol.* **20**, 1–86 (2000).
- Boskovic, D. S. et al. Structural and protein preservation in fossil whale bones from the Pisco formation (middle-upper Miocene), Peru. *Palaios* **36**, 155–164. <https://doi.org/10.2110/palo.2020.032> (2021).
- Cadena, E. A. In situ SEM/EDS compositional characterization of osteocytes and blood vessels in fossil and extant turtles on untreated bone surfaces; different preservational pathways microns away. *PeerJ* **8**, e9833. <https://doi.org/10.7717/peerj.9833> (2020).
- Longo, S., Riccio, M. & McCune, A. R. Homology of lungs and gas bladders: Insights from arterial vasculature. *J. Morphol.* **274**, 687–703. <https://doi.org/10.1002/jmor.20128> (2013).
- Cupello, C. et al. Allometric growth in the extant coelacanth lung during ontogenetic development. *Nat. Commun.* **6**, 8222. <https://doi.org/10.1038/ncomms9222> (2015).
- Cupello, C., Meunier, F. J., Herbin, M., Clément, G. & Brito, P. M. Lung anatomy and histology of the extant coelacanth shed light on the loss of air-breathing during deep-water adaptation in actinistians. *R. Soc. Open Sci.* **4**, 161030. <https://doi.org/10.1098/rsos.161030> (2017).
- Cupello, C. et al. Lung evolution in vertebrates and the water-to-land transition. *Elife* **11**, e77156. <https://doi.org/10.7554/eLife.77156> (2022).
- Cupello, C. et al. The homology and function of the lung plates in extant and fossil coelacanths. *Sci. Rep.* **7**, 1–8. <https://doi.org/10.1038/s41598-017-09327-6> (2017).
- Millot, J., Anthony, J. & Robineau, D. *Anatomie de Latimeria chalumnae III* (CNRS, 1978).
- Perry, S. F., Wilson, R. J. A., Straus, C., Harris, M. B. & Remmers, J. E. Which came first, the lung or the breath?. *Comp. Biochem. Physiol.* **129**, 37–47. [https://doi.org/10.1016/S1095-6433\(01\)00304-X](https://doi.org/10.1016/S1095-6433(01)00304-X) (2001).
- Brito, P. M., Meunier, F. J., Clément, G. & Geffard-Kuriyama, D. The histological structure of the calcified lung of the fossil coelacanth *Axelrodichthys araripensis* (Actinistia: Mawsoniidae). *Palaeontology* **53**, 1281–1290. <https://doi.org/10.1111/j.1475-4983.2010.00998.x> (2010).
- Tissier, J., Rage, J. C. & Laurin, M. Exceptional soft tissues preservation in a mummified frog-eating Eocene salamander. *PeerJ* **5**, e3861. <https://doi.org/10.7717/peerj.3861> (2017).
- Wang, X. et al. *Archaeorhynchus* preserving significant soft tissue including probable fossilized lungs. *PNAS* **115**, 11555–11560. <https://doi.org/10.1073/pnas.1805803115> (2018).
- Rossi, V., McNamara, M. E., Webb, S. M., Ito, S. & Wakamatsu, K. Tissue-specific geometry and chemistry of modern and fossilized melanosomes reveal internal anatomy of extinct vertebrates. *PNAS* **116**, 17880–17889. <https://doi.org/10.1073/pnas.1820285116> (2019).
- Cupello, C., Clément, G. & Brito, P. M. Evolution of air breathing and lung distribution among fossil fishes. In *Evolution and Development of Fishes* (ed. Johanson, Z.) 252–262 (Cambridge University Press, 2019).
- Owen, R. *Lectures on the Comparative Anatomy and Physiology of the Vertebrate Animals, delivered at the Royal College of Surgeons of England, in 1844 and 1846* 308 (Longman, Brown, Green and Longmans, 1846).
- Darwin, C. *The Origin of Species by Means of Natural Selection* 502 (Murray, 1859).
- Cass, A. N., Servetnick, M. D. & McCune, A. R. Expression of a lung developmental cassette in the adult and developing zebrafish swimbladder. *Evol. Dev.* **15**, 119–132. <https://doi.org/10.1111/ede.12017> (2013).
- Cui, J. et al. Transcriptome analysis of the gill and swimbladder of Takifugu rubripes by RNA-Seq. *PLoS One* **9**, e85505 (2014).
- Daniels, C. B. et al. The origin and evolution of the surfactant system in fish: Insights into the evolution of lungs and swim bladders. *Physiol. Biochem. Zool.* **77**, 732–749 (2004).
- Goodrich, E. S. Studies on the structure and development of vertebrates. *J. Nerv. Ment. Dis.* **74**, 678. <https://doi.org/10.1097/00005053-193111000-00026> (1931).
- Perry, S. F. & Sander, M. Reconstructing the evolution of the respiratory apparatus in tetrapods. *Respir. Physiol. Neurobiol.* **144**, 125–139. <https://doi.org/10.1016/j.resp.2004.06.018> (2004).
- Neumayer, L. Die entwicklung des darms von acipenser. *Acta Zool.* **11**, 39–150. <https://doi.org/10.1111/j.1463-6395.1930.tb00123.x> (1930).
- Wassnetzov, W. Über die morphologie der schwimmlase. *Zool. Jahrb. Allg. Zool.* **56**, 1–36 (1932).

28. Zheng, W. *et al.* Comparative transcriptome analyses indicate molecular homology of zebrafish swimbladder and mammalian lung. *PLoS One* **6**, e24019. <https://doi.org/10.1371/journal.pone.0024019> (2011).
29. Liem, K. F. Form and function of lungs: The evolution of air breathing mechanisms. *Am. Zool.* **28**, 739–759. <https://doi.org/10.1093/icb/28.2.739> (1988).
30. Funk, E., Lencer, E. & McCune, A. Dorsal-ventral inversion of the air-filled organ (lungs, gas bladder) in vertebrates: RNA sequencing of laser capture microdissected embryonic tissue. *J. Exp. Zool. B* **334**, 325–338. <https://doi.org/10.1002/jez.b.22998> (2020).
31. Nulens, R., Scott, L. & Herbin, M. An updated inventory of all known specimens of the *Coelacanth Latimeria* spp. *S. Afr. Inst. Aquat. Biodivers.* **3**, 1–52 (2011).
32. Paganin, D., Mayo, S. C., Gureyev, T. E., Miller, P. R. & Wilkins, S. W. Simultaneous phase and amplitude extraction from a single defocused image of a homogeneous object. *J. Microsc.* **206**, 33–40. <https://doi.org/10.1046/j.1365-2818.2002.01010.x> (2002).

Acknowledgements

We are especially grateful to the editor S. Stumpf and the anonymous referees for their valuable comments. We are grateful to E. Bernard (Curator of Palaeobiology, Natural History Museum, Earth Science, United Kingdom) for providing access to the fossil fish collection and for the loan of the *Macropoma mantelli* specimen. X-ray tomography scans of *Macropoma mantelli* were performed at the X-ray Tomography Imagery Platform AST-RX, 'Plateau technique d'Accès Scientifique à la Tomographie à Rayons X', MNHN, Paris, France (funded by MNHN, CNRS, Institut de France, Région Île-de-France). We thank M. Garcia Sanz for the X-ray tomography scans and F. Goussard for support at the 3D Imaging facilities of the CR2P laboratory. Thanks are also due to L. Cazes for the photography of specimen CCC 79. Synchrotron experiments were performed on the ID19 beamline at the European Synchrotron Radiation Facility (ESRF), Grenoble, France. We are grateful to P. Tafforeau at ESRF for assistance during the experiment.

Author contributions

Study Concept and Design: C.C. Acquisition of Data: C.C., G.C, M.H. Analysis and Interpretation of the Data: C.C., G.C., M.H., F.J.M., and P.M.B. Writing original draft: C.C. Reviewing and editing the draft: C.C., G.C., M.H., F.J.M, and P.M.B. All authors have read and agreed to the published version of the manuscript.

Funding

C.C. research was supported by Coordenação de Aperfeiçoamento de Pessoal de Nível Superior—Brasil (CAPES)—grant Finance Code 001 (Programa Nacional de Pós Doutorado-PNPD); Programa de Apoio à Docência (PAPD) grant (E-26/007/10661/2019)—Universidade do Estado do Rio de Janeiro; and FAPERJ grants E-26/200.605/2022; E-26/210.369/2022. P.M.B research was supported by CNPq grant 305118/2021-8 and FAPERJ 26/201.172/2022.

Competing interests

The authors declare no competing interests.

Additional information

Supplementary Information The online version contains supplementary material available at <https://doi.org/10.1038/s41598-024-61065-8>.

Correspondence and requests for materials should be addressed to C.C.

Reprints and permissions information is available at www.nature.com/reprints.

Publisher's note Springer Nature remains neutral with regard to jurisdictional claims in published maps and institutional affiliations.



Open Access This article is licensed under a Creative Commons Attribution 4.0 International License, which permits use, sharing, adaptation, distribution and reproduction in any medium or format, as long as you give appropriate credit to the original author(s) and the source, provide a link to the Creative Commons licence, and indicate if changes were made. The images or other third party material in this article are included in the article's Creative Commons licence, unless indicated otherwise in a credit line to the material. If material is not included in the article's Creative Commons licence and your intended use is not permitted by statutory regulation or exceeds the permitted use, you will need to obtain permission directly from the copyright holder. To view a copy of this licence, visit <http://creativecommons.org/licenses/by/4.0/>.

© The Author(s) 2024